Structures of Nanoparticles Prepared from Oil-in-Water Emulsions[1]

Brita Sjöström,[2,5,6] Alon Kaplun,[3] Yeshayahu Talmon,[3] and Bernard Cabane[4]

Received January 13, 1994; accepted August 26, 1994

Hydrophobic substances were dissolved in an organic solvent and emulsified with an aqueous solution at very high shear. Droplets of very small sizes (50–100 nm) were obtained by using surfactants which were combinations of lecithins and bile salts. After emulsification, the organic solvent was removed by evaporation, yielding stable dispersions of solid particles. The sizes, shapes, and structures of the particles were examined through quasi-elastic light scattering, small-angle neutron scattering and cryotransmission electron microscopy. Cholesteryl acetate particles stabilized by lecithin and bile salts were found to be platelets of 10–20 nm thickness and 80 nm diameter. Cholesteryl acetate particles stabilized with POE-(20)-sorbitan monolaurate were dense spherical globules of diameter 100 nm. Particles with a composition similar to the endogenously occurring lipoprotein, LDL, were large spherical globules studded with small vesicles. The subsequent evolution of the cholesteryl acetate dispersion upon aging was examined. There was no transfer of cholesteryl acetate between particles nor to large crystals. However, some aggregation of the particles was observed when the volume fraction of the particles in the aqueous dispersion exceeded 0.05. Thus, the structure of the nanoparticles obtained through deswelling of emulsion droplets changes according to the nature of the emulsifiers and to the composition of the hydrophobic substances which they contain.

KEY WORDS: nanoparticles; cholesteryl acetate; o/w emulsions; cryo-transmission electron microscopy; small angle neutron scattering.

INTRODUCTION

Many drugs currently under development are large polycyclic molecules which have very low solubility in water. Administration of these drugs through the parenteral route is prohibited if there is a risk that drug crystals may block blood vessels. Administration through the oral route is inefficient because only low amounts of the drug dissolve in the gastro-intestinal liquid and cross the epithelial barrier. Therefore there is a need for delivery systems that are adapted to carrying hydrophobic substances.

Usual delivery systems are emulsions (1-3), liposomes (4, 5), micelles (6, 7) and polymer particles (8, 9). In all these systems the drug is dissolved in a carrier which is a surfactant, a lipid, or an oil emulsified with surfactants. The amount of drug that may be dissolved at equilibrium in such systems is limited by the intrinsic solubility of the drug in the carrier, which is on the order of 10% (10). Thus, administration of the drug through such systems is limited by the large ratios of carrier to drug that must be used. In some cases this may be a problem, for instance in cases where large amounts of drug need to be delivered.

Carrier-free delivery systems are based on the principles of dispersing pure drug in water, either as solid particles or as liquid droplets, with only small amounts of surfactants or macromolecules used to ensure the colloidal stability of the dispersion.

The main constraint on such dispersions concerns the particle sizes. For parenteral administration, the particle sizes must be well below 5 μm, otherwise they may lead to pulmonary embolism. For oral administration, fast dissolution of the drug particles requires particles with 10 to 100 m^2/g of surface area, leading to sizes in the order of 100 to 10 nm. The content of the particles should be as close as possible to the pure drug, and free of solvent residues. Finally it would be necessary to obtain stable dispersions, exempt of processes that lead to particle growth or aggregation.

In this work we prepared particles of a model hydrophobic substance, cholesteryl acetate, and also of mixtures of hydrophobic lipids and steroids. These substances were chosen because of their very low solubility in water, and also because they are very well characterized. The preparation of the particles is based on dissolution of the drug in a volatile solvent, high shear emulsification and evaporation of the solvent, as described previously (11, 12). However, the acceptability of such dispersions as drug delivery systems depends on characterization of the particle structure and properties. The work presented here was aimed at characterizing the particle structures, and examining how these structures may vary according to the components of the particles.

In order to fully characterize the particle structures, we used a combination of direct methods (microscopy) and indirect methods (scattering). Direct methods provide qualitative information (images) on the shape and structure of the particles. Indirect methods measure geometrical parameters which provide a quantitative determination of particle structure. To our knowledge, this combination of methods has not been applied before to nanometric emulsions and dispersions. The results of this analysis demonstrate that particle sizes, shapes and structures may vary dramatically with composition, even when the components have been chosen to provide good colloidal stability of the dispersion after preparation.

MATERIALS AND METHODS

Materials

In most experiments, cholesteryl acetate was chosen as the main component of the particles, because it is representative of sparingly soluble drugs. In some experiments, the LDL components indicated in **Table I** were used. Choles-

[1] This work used the neutron beams of LLB in Saclay, France. It was performed as part of the BIOAVENIR program financed by RHONE-POULENC with the MRE and MICE.

[2] Institute for Surface Chemistry, P.O. Box 5607, S-114 86 Stockholm, Sweden.

[3] Department of Chemical Engineering, Technion, Haifa 32000, Israel.

[4] Equipe mixte CEA-RP, Service de Chimie Moléculaire, CE-Saclay, 91191 Gif sur Yvette Cedex, France.

[5] Present address: Pharmacia Plasma Products, S-112 87 Stockholm, Sweden.

[6] To whom correspondence should be addressed.

0724-8741/95/0100-0039$07.50/0

Table I. Composition, %(w/w) of the artificial low density lipoprotein particle

Cholesterol	15.5
Cholesteryl linoleate	40.2
Cholesteryl oleate	23.9
Cholesteryl palmitate	10.6
Soybean oil	6.5
Tristearin	0.5
Tripalmitin	2.8

terol, cholesteryl acetate, cholesteryl linoleate, cholesteryl oleate, cholesteryl palmitate, tripalmitin and tristearin were obtained from SIGMA Chemical Co. Chromatographically purified soybean oil was obtained from CPLSBO, Karlhamns LipidTeknik. In addition, the emulsifiers indicated in Table II were used.

Particle Preparation

The method for preparation of the particles has been described previously (11). The water insoluble components (e.g. cholesterol, cholesteryl esters, triglycerides or lipids) were dissolved in cyclohexane or toluene. The water soluble components (e.g. bile salts or synthetic emulsifiers) were dissolved in water. The ratio of organic phase to aqueous phase was kept at 10:90.

The oil/water mixture was emulsified to form a water-continuous emulsion. A first stage of emulsion was performed in a rotor/stator mixer for 2 minutes at room temperature (Ultra Turrax T18/10). This was followed by high pressure homogenization at a 1000 bar pressure difference for about 5 minutes with cooling in an ice/water bath (Microfluidizer TM110). Finally, the organic solvent in the emulsions was removed at room temperature by evaporation in a rotavapor at a pressure of 100 mbar.

Table II. Emulsifiers used in the study

Emulsifier	Trade name (code)	HLB	Manufacturer
POE-(20)-sorbitan monolaurate	Tween 80 (T80)	15[a]	ICI
Lecithin, soybean	Epikuron 145 (E145)	6-7[a]	Lucas Meyer
Lecithin, soybean	Epikuron 170 (E170)	6-7[a]	Lucas Meyer
Lecithin, soybean	Epikuron 200 (E200)	7[b]	Lucas Meyer
Lecithin, soybean	Phospholipon®5 (P5)	6-7[b]	Natterman
Lecithin, soybean	Phospholipon®90G (P90)	7[b]	Natterman
Polyethylene glycol	(PEG 400)	10[b]	Hoechst
Polyoxyethylene-polyoxypropylene	Pluronic 127NF (P127NF)	18-23[a]	BASF Wyandotte Corp.
Sodium salt of glocholic acid	(GCA)	25[b]	Sigma Chem.

[a] From the commercial source.
[b] Estimated from the water solubility of the emulsifier (29, 30)).

Analysis of Solvent Residues

The toluene content of the dispersions was determined by spectrophotometry (SP 8-200, PYE UNICAM). The dispersion was dissolved in ethanol prior to the analysis. The peak occurred at 270 nm. The cyclohexane residue in the dispersion was analysed by gas chromatography. The carrier gas was helium, the stationary phase 10% Apiezon L and the carrier Chromosorb W HP (CHROMPACK). The temperature at the injection was 100 °C, the column temperature was 70 °C, and the temperature of the flame ionization detector was 140 °C (CARLO ERBA 4200).

Cryo-Transmission Electron Microscopy (Cryo-TEM)

Thin vitrified specimens were prepared for transmission electron microscopy in a controlled environment vitrification system (CEVS), at fixed temperature and 100% relative humidity. This assured minimal changes in the specimen prior to vitrification. Thin liquid films were prepared on perforated carbon films supported on 3 mm electron microscope grids. A specimen was prepared by applying a small (about 3μl) drop onto the grid, blotting most of it to the desired thickness (under 200 nm) and plunging it into liquid ethane at its melting point. This ultra-fast cooling caused vitrification of the liquid phase, i.e., specimens became solid-like (vitreous) without change of phase that leads to structural rearrangement. These cryo-specimens were stored under liquid nitrogen, and transferred to the cooling-holder (Gatan 626) of the TEM (JEOL 2000FX), where they were equilibrated at −170°C, and examined with an acceleration voltage of 100 kV. More details about the technique are given by Bellare et al. (13). Other recent applications are presented by Clausen et al. (14), Cochin et al. (15), Laughlin et al. (16) and Kamenka et al. (17).

Quasi-Elastic Light Scattering (QELS)

Particle sizes were determined from their self-diffusion coefficients according to fluctuations in the intensity of scattered light. This technique is very well known (18, 19), but it is necessary to specify here how the analysis was carried out.

For a dispersion of monodisperse particles, the autocorrelation of the fluctuations decays as a single exponential, and the exponent is simply related to the diffusion coefficient, D, of the particles. For spherical particles the value of D may be used to calculate the particle diameter, d, through the Stokes-Einstein relation.

A particular problem arises with the determination of the sizes of anisotropic particles. The diffusion of coefficients of anisotropic particles were calculated 60 years ago by Francis Perrin (20, 21). In this calculation, the hydrodynamic diameter, d_h, can be related to the diameter, d_s, of a sphere with the same volume according to:

$$d_h = d_s / F(p) \quad (1)$$

The shape function F(p) depends only on the value of the particle anisotropy (p) defined as $p = a_1/a_2$, where a_1 is the diameter along the axis of revolution and a_2 the diameter across the equator. For spheres, F(p) is unity by definition of d_s. For prolate ellipsoids (p>1) the expression of F(p) is:

$$F(p) = p^{1/3}(p^2 - 1)^{-1/2} \ln [p + (p^2 - 1)^{1/2}] \quad (2)$$

For oblate ellipsoids (p<1) the expression for F(p) is:

$$F(p) = p^{1/3} (1 - p^2)^{-1/2} \text{ arc tan } [p^{-1} (1 - p^2)^{1/2}] \quad (3)$$

As an example, for discs of 10 nm thickness and 70 nm diameter, the diameter of spheres with the same volume is d_s = 42 nm, and the hydrodynamic diameter of the discs is d_h = 55 nm.

For polydisperse particles, the autocorrelation decay may be analyzed as a sum of exponentials, and various mean diameters may be calculated by different weighting procedures. We have calculated the volume average diameter, d_v, defined according to the numbers N_i of particles with volume v_i and diameter d_i:

$$d_v = (\Sigma N_i v_i d_i) / (\Sigma N_i v_i) = (\Sigma N_i d_i^4) / (\Sigma N_i d_i^3) \quad (4)$$

It may also be desired to find a distribution of diameters which reproduces the observed correlation function. This is an ill-defined problem and its solution is non unique. We have assessed the stability of this analysis by comparing distributions obtained on successive runs with the same sample (effect of small variations of the data on the calculated distributions), and also by comparing distributions obtained through different procedures (cumulants, NNLS and CONTIN). The results were quite stable for the finer emulsions or dispersions, that do not have excessive polydispersity, and less so for the larger "LDL" dispersions, that have broader size distributions.

Small-Angle Neutron Scattering (SANS)

The structure of the particles was examined through SANS. Neutrons are scattered by differences in scattering length between nuclei in the particles and nuclei in the continuous phase. Good contrast between particles and continuous phase was achieved using D_2O as the continuous phase. Then all regions made of hydrogenated molecules had a low density of scattering length, whereas all regions penetrated by D_2O had a high density of scattering length. Consequently the objects that were seen by neutrons were made of everything that was not penetrated by D_2O (22).

Two-dimensional scattering patterns were obtained on the instrument PAXY of LLB. These patterns were subsequently radially averaged to yield scattering curves of intensity, I, vs. magnitude, Q, of the scattering vector. Q is related to the wavelength, λ, of incident neutrons and to the scattering angle, θ, by:

$$Q = (4\pi/\lambda) \sin (\theta/2) \quad (5)$$

The general features of scattering curves for independent particles dispersed in a homogeneous continuous phase are as follows (22-25).

(a) At $Q \to 0$ the intensity, I_o, is proportional to particle mass concentration and to the square of the difference in density of scattering length, $\Delta\rho$, between D_2O and the protonated molecules in the particles. Hence, the average content of the particles may be determined.

(b) At higher Q values, the rays scattered by nuclei at opposite ends of the particle interfere destructively. In this regime, the curvature of the scattering curve measures the average radium of gyration, R_g, of the particles. This quantity may be determined by fitting the measured intensity curve to an expansion formula. For globular particles the best expansion is the Guinier formula (23):

$$I = I_o \exp (-Q^2R_g^2 /3) \quad (6)$$

For flat particles, or for bushy particles with fractal dimension $d_f \approx 2$, the best expansion is the Zimm formula (25):

$$1/I = 1/I_o (1 + Q^2R_g^2 / 3) \quad (7)$$

(c) At higher Q values, the intensity decay reflects interferences at shorter distances within each particle, i.e. their internal structure. For dense globular particles (no internal structure), the intensity follows Porod's law, from which the surface area A of the particles may be determined (24):

$$I(Q) \approx A\, Q^{-4} \quad (8)$$

For flat particles the destructive interference is not as strong, and the decay is only according to Q^{-2}; for rod-like particles it is Q^{-1}. For bushy or porous particles with fractal dimension d_f the decay follows the power law Q^{-d_f} (25). Thus, from the slope of the intensity decay in a log-log plot, the dimensionality of the particles may be determined.

RESULTS

The particles were made by evaporating volatile solvent from emulsion droplets, as explained above. During this process the droplets must deswell until the concentration of non volatile components is unity. The aim of this work was to find out whether this process can lead to different types of particles, depending on the nature of the non volatile components. For this reason, particles were made with different hydrophobic and hydrophilic components. The hydrophobic components were used to make the particle cores; they were apolar steroids, meant to represent a water-insoluble drug, or the "LDL" components listed in **Table I**. The hydrophilic components were used to cover the particle surfaces and confer colloidal stability to them; they were lecithins, bile salts or synthetic emulsifiers, all listed in **Table II**. At high concentration some of these molecules remain in a liquid state, others turn to a solid state; they also have different solubilities in the hydrophobic components. Therefore it was suspected that droplets made with different hydrophilic components may shrink to different types of particles.

Composition of the Particles

The procedure for obtaining through solvent evaporation was efficient, as the amounts of solvent residues were found to be quite small. For the "standard" dispersion made from an emulsion containing 25% cholesteryl acetate in cyclohexane, the final residue of cyclohexane was 25 ppm of the total weight of the dispersion. For dispersions made from

toluene emulsions, a systematic study was performed by changing the initial ratio of cholesteryl acetate to toluene. It was found that the amount of toluene residue decreased linearly with an increased ratio of cholesteryl acetate to toluene, from 100 ppm of the total mass of the dispersion when cholesteryl acetate was 5% of the organic phase to 20 ppm when cholesteryl acetate was 50% of the organic phase. Therefore the particles could be considered as made only from the hydrophobic and hydrophilic components listed above.

Particle Sizes for Different Lipid Mixtures

In a first step, particles were made with a lipid composition similar to the endogenously occurring lipoprotein, LDL (26). These particles consisted mainly of cholesterol, cholesteryl esters and triglycerides (**Table I**). These lipids were dissolved in a cyclohexane solution (25% w/w) containing soybean lecithins (5% w/w of P90 and P5). After emulsification with an aqueous solution the organic solvent was evaporated and the diameters of the resulting particles were measured. The average diameter measured by SANS was 130 nm, whereas that obtained from QELS was 184 nm. The discrepancy is too large to be explained by differences between diameters measured on the same particle by either method, i.e. "wet" particle diameter in QELS and "dry" diameter in SANS. It must be caused by a broad distribution of sizes of the LDL particles, where the largest sizes are out of the range accessible in SANS. Indeed, whenever narrow size distributions were observed, the QELS and SANS results were close to each other (see below).

Next, a simpler lipid composition was used, and the nature of the emulsifier was varied systematically. The hydrophobic components, a blend of cholesteryl oleate and cholesteryl palmitate (1:1), were dissolved as above in cyclohexane and emulsified using the emulsifiers listed in **Table II**. The mean diameters of the resulting particles are presented in **Table III**. The most efficient emulsifier blend, for obtaining the smallest particle size, is the mixture soybean lecithin : sodium glycocholate (E200 : GCA).

With this emulsifier mixture, a systematic study of the particles was undertaken. For this study, pure cholesteryl acetate was dissolved in cyclohexane (25% w/w), and emulsified in water with E200 : GCA (5% w/w). The size distribution of emulsion droplets was measured by QELS (Figure 1) and was found to be monomodal with a mean diameter of 66 nm. The solvent was then evaporated, and the size distribution of the resulting particles was measured as well. It was nearly identical to the distribution of emulsion droplet sizes, with a mean diameter of 58 nm (**Figure 1**). The sizes measured by SANS were 57 nm for the droplets and 46 to 55 nm for the particles (**Table IV**), respectively. These sizes are quite close to those obtained by QELS, as expected from the narrow size distributions.

Particle Size vs. Emulsion Droplet Size

The match between the sizes of emulsion droplets and the sizes of resulting particles is remarkable, since the content of the particles is much reduced by the evacuation of organic solvent. The relation between the emulsion droplet size and the particle size was investigated quantitatively with different particle sizes. For this study, toluene was chosen as the organic carrier since the concentration of cholesteryl acetate in toluene may be varied over a wide range, up to 53% w/w. Accordingly, emulsions were made containing 5 to 50% cholesteryl acetate in toluene, and stabilized by the surfactant POE-(20)-sorbitan monooleate. Different concentrations of surfactant were used to obtain different emulsion

Table III. Particle sizes obtained with different types of emulsifiers. First row: nature of the emulsifier (details in Table I). Second row: mean hydrodynamic diameter of the particles (nm), as measured by QELS. The dispersed phase of the emulsion was made from a 4:1 mixture of cholesteryl oleate/cholesteryl palmitate dissolved at 25% (w/w) in cyclohexane. The emulsifier concentration was 5% (w/w) calculated on the basis of the dispersed phase of the emulsion

Emulsifier	Particle diameter (nm)
E145	162, 187
E 170	225
E145 /P127NF	190
E170 /P127NF	260
E200 /P127NF	205
E145 /PEG400	125
E170 /PEG400	180
E200 /PEG400	200
E145 /T80	120, 220
E170 /T80	305
E145 /GCA	75, 100
E170 /GCA	100

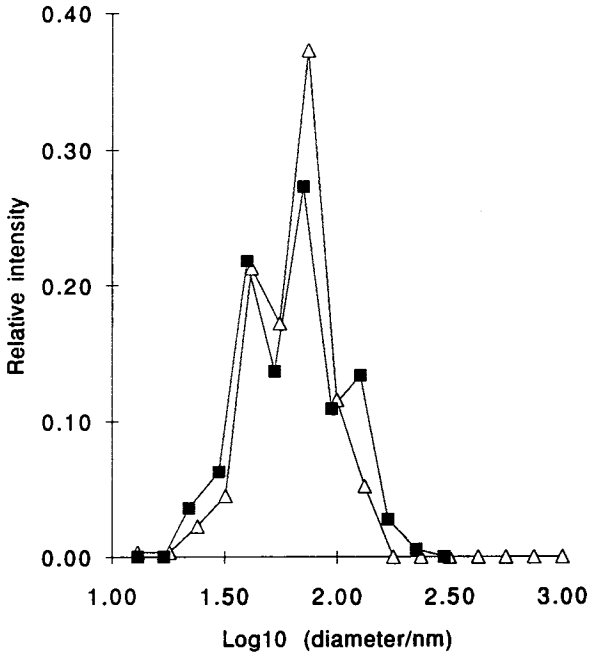

Figure 1. Size distributions for emulsion droplets (triangles) and for the particle derived from them (squares). Verical scale: relative intensities from QELS. Horizontal scale: Log_{10} (mean hydrodynamic diameter in nm). The dispersed phase of the emulsion was made from cholesteryl acetate dissolved at 25% (w/w) in cyclohexane. The emulsifier was E200:GCA in a ratio 4:1; the emulsifier concentration was 5% (w/w) of the dispersed phase of the emulsion.

Table IV. Mean diameters for cholesteryl acetate emulsions and dispersions stabilized by sodium glychocholate and soybean lecithin, in nm

Sample	Emulsion dilute	Dispersion dilute	Dispersion concentrated fresh	Dispersion concentrated stored
SANS diameter eq /6/	57	46		
SANS diameter eq /7/		55	66	90
QELS popula-tions	66	58	56 and 422	40 and 113

SANS diameter: The curvature of the neutron scattering curve was fitted according to either equation /6/ or equation /7/, and used to determine the radius of gyration, R_g, of a droplet or particle. The outer diameter was then calculated as $(20/3)^{1/2}\ R_g$.
QELS populations: Mean values for the hydrodynamic diameters of the populations observed by quasi-elastic light scattering.

droplet sizes. There was a 1:1 correlation between the initial emulsion droplet size and the obtained particle size, as long as the cholesteryl acetate concentration in toluene was above 10%, and provided that the emulsion was stable (Figure 2). For smaller contents of cholesteryl acetate the particle sizes were smaller (Figure 2, filled squares), but the reduction was not as large as anticipated from the loss of solvent (full line).

With smaller amounts of emulsifier the particles were larger but the effect was the same (Figure 2). However, at the lowest emulsifier concentration (1% in toluene) the particles turned out to be larger than the initial droplet size. This discrepancy was a result from droplet coalescence during solvent evaporation.

Thus the sizes of emulsion droplets and of the corresponding particles may be compared only under conditions where the dispersions are well stabilized against aggregation. Under such conditions the cholesteryl acetate particle size is proportional to the emulsion droplet size. Moreover, when the "drug" concentration in the organic solvent is close to saturation, the ratio is close to unity. This phenomenon is independent of the nature of the organic solvent, e.g. cyclohexane and toluene (16). It is also independent of the choice of emulsifier and of emulsifier concentration, as long as it is sufficient to stabilize the emulsion (16). This phenomenon is also contrary to expectations, since a substantial reduction in particle volume was anticipated from the loss of organic solvent.

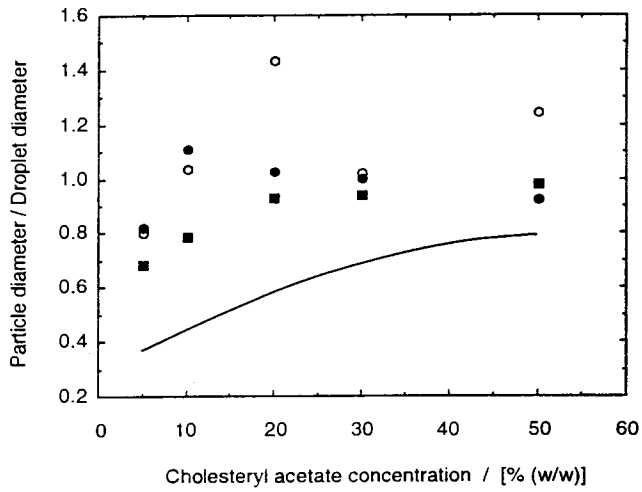

Figure 2. Shrinkage of emulsion droplets upon extraction of organic solvent. Vertical scale: particle size divided by emulsion droplet size. Horizontal scale: concentration of cholesteryl acetate in the dispersed organic phase (toluene). The emulsifier concentration (POE-20-sorbitan monooleate) was (open circles) 1% (w/w), (filled circles) 3% (w/w), and (filled squares) 10% (w/w) calculated on the basis of the dispersed organic phase. Full line: theoretical shrinkage for dense spheres.

Particle Structure from Neutron Scattering

As explained in "METHODS", the internal structure of particles may be determined from the high Q decay in small angle neutron scattering. Here the main question is the difference with regard to internal structure between the initial emulsion droplets and the resulting particles. This comparison is presented in Figure 3 for the cholesteryl acetate particles stabilized by the bile salt/lecithin mixture. The emulsion droplets give a Q^{-4} decay at high Q, which is the classical behavior for dense globular particles. Since the contrast is between D_2O and all hydrogenated materials (cyclohexane, cholesteryl acetate, emulsifiers), this implies that the

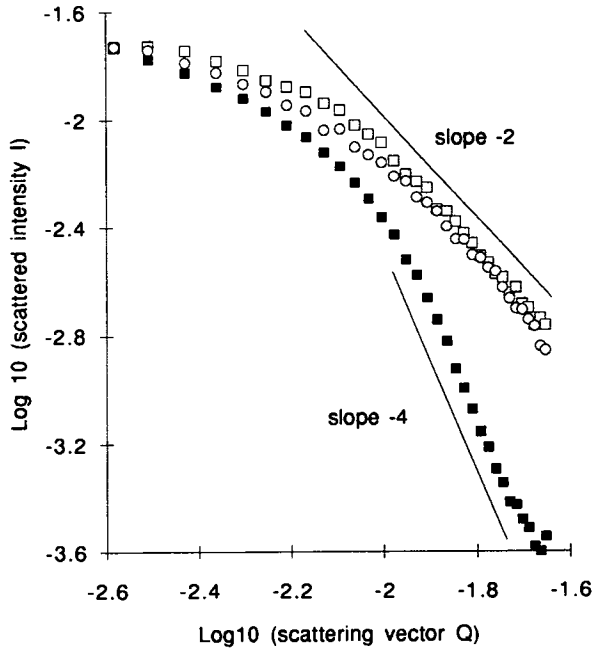

Figure 3. Neutron scattering curves for emulsions and dispersions. Vertical scale: Log_{10} (scattered intensity) for the original emulsion (filled squares), the dilute dispersion (open squares) and a concentrated dispersion (open circles). Horizontal scale: Log_{10} (scattering vector Q in $Å^{-1}$). THe cholesteryl acetate concentration was 25% (w/w) in cyclohexane, and the emulsifier (E200:CGA) concentration was 5% (w/w) of the dispersed phase of the emulsion.

entire droplet scatters as a dense sphere. The particles give a Q^{-2} decay at high Q; this implies that they are either flat (disk-like), hollow or porous. If the structure is porous, then the pores must be filled with D_2O, in order to have contrast with respect to the rest of the particle.

The scattering curves for the LDL particles are shown in Figure 4. These show a steep curvature at low Q, then a Q^{-4} decay over most of the Q range, and finally a slower decay in the high Q limit. The steep curvature at low Q reflects the large size of the particles. The Q^{-4} decay indicates that these particles are dense globules. The slower decay in the high Q limit must be caused by the scattering from much smaller objects which coexist with or within the LDL particles. These small objects might be liposomes made of excess emulsifier, or they might be pores within the particles.

Particle Microstructure from Cryo-transmission Electron Microscopy

Cryo-TEM has provided us with direct images of dispersed systems without staining and drying, and with utmost control of the conditions prior the cooling. Freezing artifacts are excluded due to vitrification. Contrary to freeze-fracture replication, in direct cryo-TEM it is much easier to distinguish between objects of similar geometrical projections (e.g., between discs and spheres), and between crystalline and non-crystalline objects.

Figure 5a shows a vitrified specimen of a cholesteryl acetate emulsion stabilized by the lecithin/sodium glycocholate blend. The volume fraction of dispersed phase was 8%, the concentration of cholesteryl acetate in the oil phase

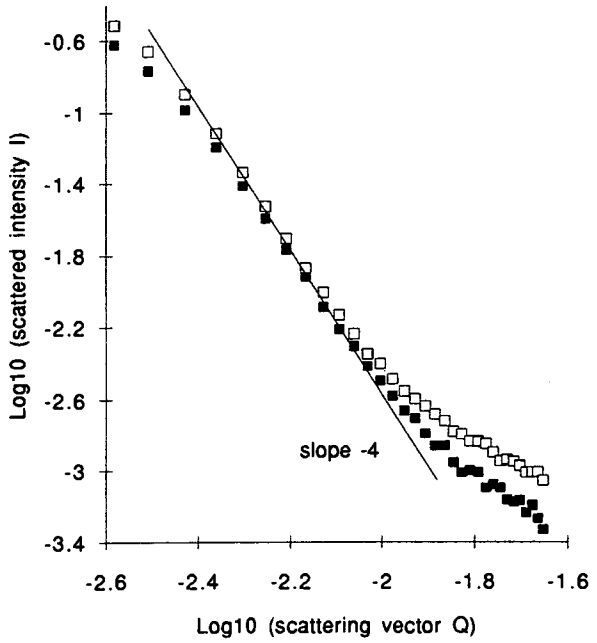

Figure 4. Neutron scattering curves of artifical LDL particles in the original dispersion (filled squares) and in the stored concentrated dispersion (open squares). The particles were made from a 25% solution of "drug" (Table II) in cyclohexane emulsified in water with a mixture of P90 and P5 (concentration of emulsifiers 5% (w/w) calculated on the dispersed phase of the emulsion).

was 25% (w/w) and the concentration of emulsifier was 5% (w/w) calculated on the dispersed phase of the emulsion. The micrograph shows the droplets of "oil" in the continuous water phase. The rather uniform optical density throughout the particles indicates drops, not vesicles. Vesicle and liposome images by the same technique have been shown in Walter et al. (27) and Laughlin et al. (20). See also Figure 5c. The faint halos around the particles are Fresnel fringes, a result of the approximately 4 μm underfocus of the objective lens, used to enhance image contrast.

Figure 5b shows cholesteryl acetate particles in a 2% dispersion prepared from the emulsion stabilized by the lecithin/sodium glycocholate blend. The particles were pushed and concentrated in one area of the liquid film by the blotting used in sample preparation (28). The appearance of the disks suggests platelets. This is deduced from the fact that the different sized discs have the same optical densities, whereas smaller spheres would look fainter than larger ones. Some of the platelets are seen edge-on, looking in projection like cylinders. In Figure 5c many more edge-on views of platelets can be seen. Here, two rather large vesicles are also observed.

The lack of any crystalline contrast effects in the particles, such as bend contours, stacking faults or dislocations, and the apparent flexibility of the platelets suggest that they are in fact not crystalline.

Figure 6 shows a vitrified specimen of a 2% cholesteryl acetate dispersion made from an emulsion stabilized with the sorbitan ester, with the same concentrations as the previous dispersion. The micrograph shows spherical particles in the continuous water phase.

Figure 7a shows a vitrified specimen of an 8% emulsion containing 25% (w/w) of the "LDL" lipid mixture stabilized with lecithin. The emulsifier concentration was 5% (w/w) calculated on the basis of the dispersed phase of the emulsion. The micrograph shows the droplets of "oil" in the continuous water phase. There are small vesicles adsorbed on the surface of the emulsion droplets. Figure 7b shows the particles obtained after removal of the organic solvent from the emulsion. The morphology of the particles is similar to the emulsion droplet structure according to the cryo-TEM micrograph.

Structural Evolution on Storage

Dispersions of fine particles are susceptible to spontaneous evolution where the size of dispersed particles grows, leading to a degradation of the properties of the dispersion. With nanometric dispersions this problem is serious, because the drive for reduction in surface areas is quite strong. There are two processes through which this evolution may occur: aggregation of particles, and transfer of mass from particles to large crystals. The possible occurrence of these processes was examined for the cholesteryl acetate dispersions.

In a first step, the effects of aging processes were examined through light scattering. In dilute dispersions (volume fraction <0.03) of cholesteryl acetate particles stabilized by the glychocholate/lecithin emulsifiers, the particle sizes were found to be stable over time (storage at 5C for 40 days). In concentrated dispersions obtained through evapo-

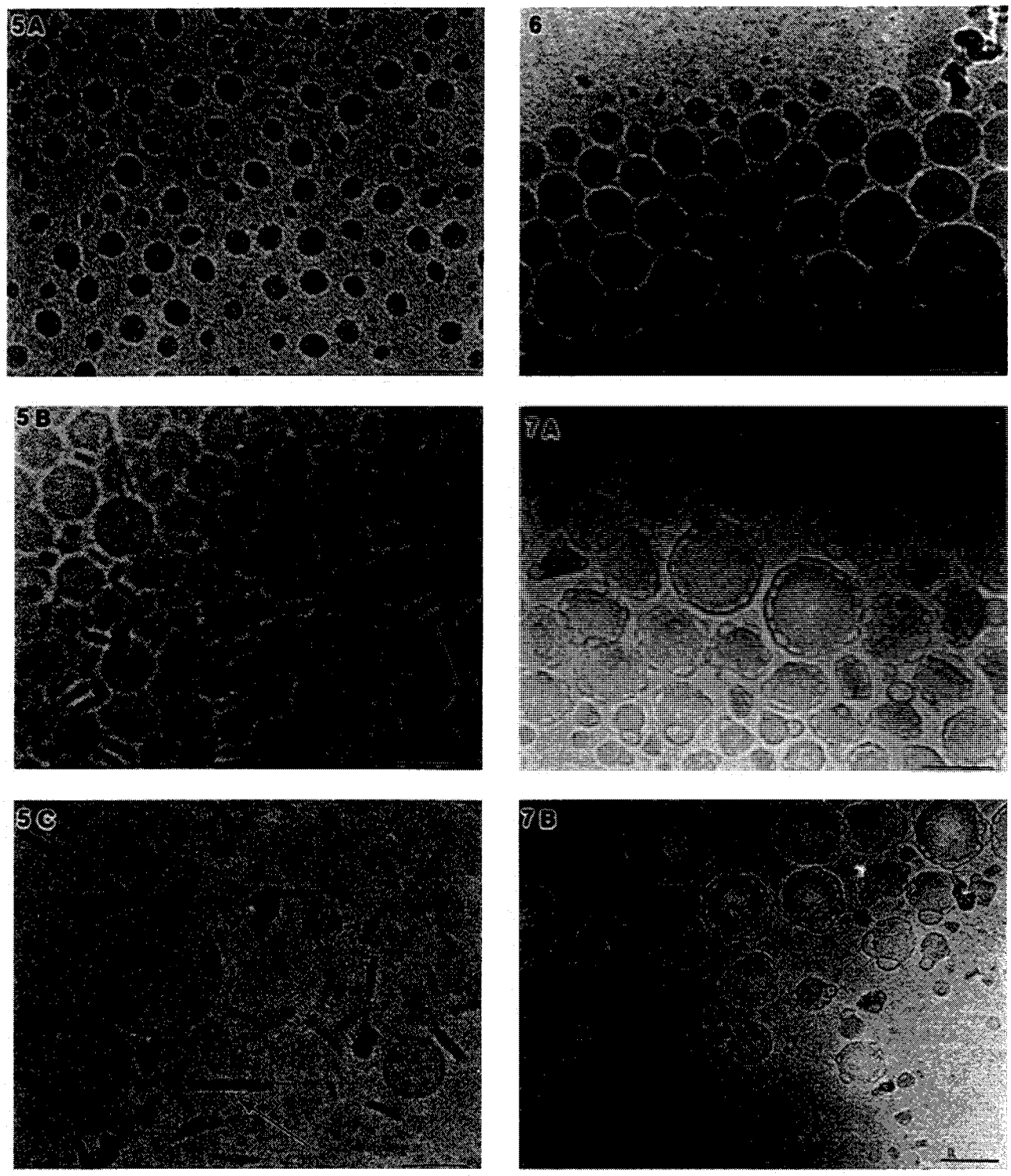

Figure 5. Cryo-transmission electron microscopy images of a cholesteryl acetate emulsion made with the emulsifier E200:CGA, (A), and of the corresponding cholesteryl acetate dispersion, (B,C). Arrows in (B) and (C) indicate edge-on views of cholesteryl acetate platelets. Bars correspond to 100 nm.

Figure 6. Cryo-transmission electron microscopy image of a cholesteryl acetate dispersion made with the emulsifier POE-20-sorbitan monooleate. Bar corresponds to 100 nm.

Figure 7. Cryo-transmission electron microscopy image of a cyclohexane emulsion containing a lipid mixture (A) and the resulting artifical LDL particles (B). Bar corresponds to 100 nm.

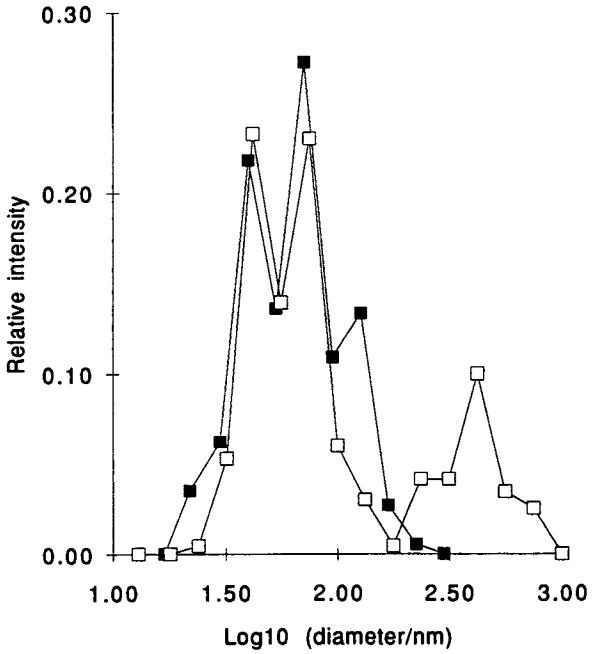

Figure 8. Size distributions for stored concentrated dispersions (open squares) compared with the original dispersions (filled squares). Vertical scale: relative intensities from QELS. Horizontal scale: Log_{10} (mean hydrodynamic diameter in nm). The second population centered at 400 nm results from aggregation of primary particles in the population at 50 nm.

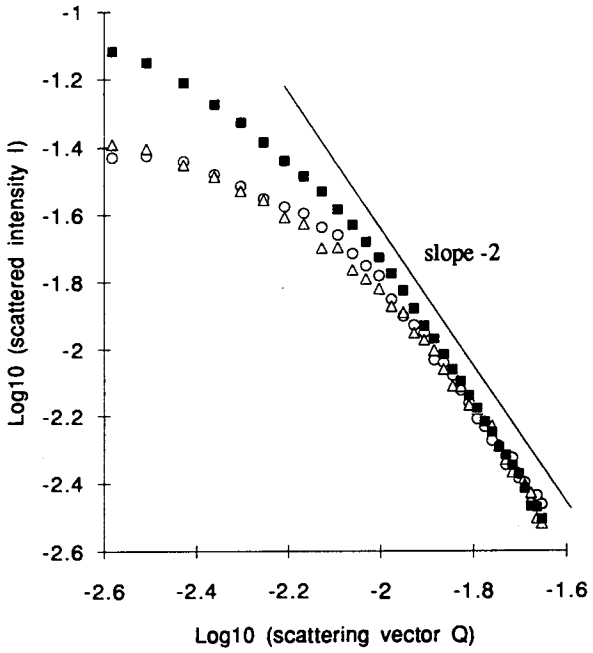

Figure 9. Aging of the dispersions upon storage. Neutron scattering curves of a dilute cholesteryl acetate dispersion (circles), a concentrated dispersion (triangles), and a stored concentrated dispersion (squares).

ration to a volume fraction of 0.06, there was an additional population with a mean diameter of 400 nm (Figure 8). In dispersions stored at this concentration, the latter population became dominant. From these results alone it was not possible to determine whether this growth occurred through aggregation or through transfer of mass to large crystals.

In neutron scattering experiments, such evolutions may be recognized according to changes in the low Q and in the Q parts of the scattering curves. Aggregation causes the formation of larger objects made of many individual particles. Because these objects are large, the intensity scattered at Q—>0 rises; because they are made of individual particles the intensity scattered at high Q, which describes the local structure, remains unchanged. Transfer of mass to large crystals has a similar effect on the intensity scattered at Q—>0; however, since these crystals have a reduced surface area, the asymptotic limit of the intensity must drop and follow the law for dense objects, equation /8/.

Figure 9 presents the scattering curves of the same three dispersions. At low Q, where intensities reflect the overall contents and sizes of these objects, the three curves differ. In particular, the aged concentrated dispersion shows higher intensities and a steeper curvature, confirming the presence of larger objects (Table IV). However, at high Q (scale 2-10nm), the asymptotic slopes are identical and according to Q^{-2}, indicating that the building blocks are the same flat particles in all three dispersions. The concentrated dispersions thus contained aggregates of primary particles that were irregularly bound to each other. There was no transfer of mass to larger crystals with a reduced surface area.

DISCUSSION

Nanoparticles of hydrophobic substances have been prepared in water, and they have been examined through 3 techniques: QELS, SANS and cryo-TEM. This combination of scattering and imaging techniques has not been applied before to nanoparticles, and it provides a unique opportunity to determine particle structures in an unambiguous way. Each technique indicates that the particle sizes, shapes and structures do change according to the nature of the emulsifiers used in the preparation of the particles. This general result must be discussed in three stages. First, for each dispersion, the results obtained through different techniques must be compared. Then, these results may be used to determine the processes by which the dispersions were formed. Finally, the limitations set by these processes for the generation of other nanoparticles may be evaluated.

Structures According to Scattering and Imaging Techniques

Most of the work was performed on emulsions and dispersions containing pure cholesteryl acetate as the hydrophobic ingredient and a bile salt/lecithin mixture as an emulsifier. It was verified that the emulsion droplets were well protected by this mixture and did not aggregate upon evaporation of the solvent. Therefore the experiments probed individual droplets and particles. The particle sizes were determined through QELS and SANS. The basic result is that these sizes are close to the sizes of the original emulsion droplets. However the volumes of these particles must be much smaller than those of emulsion droplets, since the solvent had been removed. Consequently they cannot be dense spheres.

The SANS curves confirm that the particles are not dense spheres. According to the high Q slope of the scattering curves they may be flat, hollow or porous. Cryo-TEM micrographs reveal that the particles are platelets. The largest dimensions of these platelets match the diameters of the original emulsion droplets, with approximately the same size distribution. The thickness, 10 to 20 nm, is surprisingly uniform.

These values are compatible with the measured hydrodynamic diameters. For instance, an emulsion droplet of diameter 66 nm, as measured, will shrink through evaporation to a particle having a volume 4 times smaller. The volume of this particle can be matched by a disk of thickness 10 nm and outer diameter 70 nm. The hydrodynamic diameter of this disk is d_h = 55 nm, close to the measured particle diameter, 58 nm (Table IV).

The same three techniques were applied to emulsions and dispersions containing cholesteryl acetate as the hydrophobic ingredient and Tween 80 as an emulsifier. In this case the protection of droplets and particles was not as good, and some aggregation was observed. Nevertheless, it was possible to examine individual droplets and particles. For the particles, the SANS curves show a Q^{-4} decay at high Q, which is typical of dense particles, and the Cryo-TEM micrographs show dense globular particles. Thus, both techniques indicate that emulsion droplets stabilized by Tween 80 shrink to dense particles upon evaporation of the solvent.

Still another morphology was obtained with the LDL composition. In this case, cryo-TEM images show that both emulsion droplets and particles were large spherical objects covered by small vesicles. SANS curves show the Q^{-4} decay from dense, globular objects, and a slower decay at the high Q end from smaller objects with excess surface area; these smaller objects may well be the vesicles seen in cryo-TEM. The size distribution of the large objects is quite broad, and, as explained in RESULTS, it is sampled differently by the three techniques.

Deswelling and Aging Processes

At this stage it is necessary to examine how different particle structures may be obtained through evaporation of volatile solvent from emulsion droplets which are all spherical. This is a deswelling process, whereby the concentration of non volatile components is increased until it reaches unity. This process is perturbed by the limited solubility of the hydrophobic components (e.g. the "drug") in the remaining solvent. For instance the limit of solubility of cholesteryl acetate in cyclohexane at 20 °C is 28% (w/w). Beyond this limit, the hydrophobic components may precipitate and separate out of the solvent. How this separation takes place determines the final structure of the particles.

In this work we have observed different outcomes for the deswelling, depending on the nature of the components. Particularly striking is the difference between the evolution of cholesteryl acetate/cyclohexane droplets stabilized by TWEEN 80, and that of similar droplets stabilized by the bile salt/lecithin mixture. The former shrink to dense globules, whereas the latter turn to platelets with a regular thickness. The main difference between both compositions is that TWEEN 80 is too hydrophilic to dissolve in the oil phase of the emulsion, whereas lecithin dissolves readily in an oil phase. Moreover, it is known that lecithin/oil/water systems may form inverted micelles or liquid crystalline phases. Therefore there is a possibility that a lamellar liquid crystal phase may have formed during the deswelling; it may even be that some of the cholesteryl acetate was dissolved in this phase. Thus, the platelet shape of the particles may originate from the formation, at some stage of the deswelling of a liquid crystal phase.

After deswelling the particles may still evolve, either by mass transfer to large crystals or by aggregation. Mass transfer, which is similar to the Ostwald ripening of emulsions, was not observed in this work. This is obviously because the solubility of cholesteryl acetate in water is extremely low (on the order of 10^{-8} w/w). Aggregation was observed at low concentration (0.03 w/w) in the dispersions stabilized with Tween 80, and also at higher concentration (0.06) in the dispersions stabilized by the bile salt/lecithin mixture. The occurrence of aggregation at volume fractions which are not very high is contrary to classical theories of colloidal stability; for instance the electrostatic barriers generated by the adsorption of the bile salt molecules on 50 nm particles may be calculated through the DLVO theory; they are on the order of 200 kT. This problem is often encountered in nanometric dispersions.

The use of such nanoparticles as carriers for drugs that are sparingly soluble in water will be limited mainly by these aging processes. Many drugs currently under development have a solubility in water which is quite low, but not as low as that of cholesteryl acetate. With a solubility above 10^{-5} w/w, transfer of mass from the particles to large crystals may occur, and degrade the properties of the dispersions. An obvious way to avoid this problem is to eliminate the continuous phase through freeze-drying after the preparation of the particles. However our results demonstrate that the particles may aggregate during this concentration process. Therefore it will be necessary to devise better surface protection in order to obtain dispersions that could be concentrated, dried and stored without degradation.

ACKNOWLEDGMENTS

The work done at the Technion was supported by grants from the United States–Israel Binational Science Foundation (BSF), Jerusalem, and from The Fund for the Promotion of Research at the Technion.

REFERENCES

1. M. Y. Levy and S. Benita. "Design and characterization of a submicronized o/w microemulsion of diazepam for parenteral use" *Int. J. Pharm.*, 54: 103–112, 1(1989)
2. R. J. Prankerd and V. I. Stella, "The use of oil-in-water emulsions as a vehicle for parenteral drug administration" *J. Parent. Sci. Technol.*, 44: 139–149, (1990)
3. L. Illum, P. West, C. Washington, and S. S. Davis. "The effect of stabilizing agents on the organ distribution of lipid emulsions" *Int. J. Pharm.*, 54: 41–49 (1989)
4. M. J. Ostro (ed.), *Liposomes. From Biophysics to Therapeutics*, Marcel Dekker, New York 1987
5. S. M. Moghimi, C. J. H. Porter, L. Illum and S. S. Davis. "The effect of Poloxamer 407 on liposome stability and targeting to bone marrow. Comparison with polystyrene microspheres" *Int. J. Pharm.*, 68: 121–126 (1991)

6. S. H. Yalkowsky (ed.), *Techniques of Solubilization of Drugs*, Marcel Dekker, New York, 1981
7. O. Von Dardel, C. Mebius and T. Mossberg. "Diazepam in emulsion for intravenous usage" *Acta Anaesth. Scand.*, 20: 221–224, (1976)
8. Vanderhoff et al. "Polymer emulsification processes" *U.S. Patent* 4: 177, 177 (1979)
9. R. Gurny, N. A. Peppas, D. D. Harrington and G. S. Banker. "Development of biodegradable and injectable latices for controlled release of potent drugs" *Drug. Dev. Ind. Pharm.* 7: 1–25 (1981)
10. R. H. Müller. "*Colloidal Carriers for Controlled Drug Delivery*" CRC press, Stuttgartt (1991)
11. B. Sjöström, Br. Kronberg and J. Carlfors. "A method for the preparation of submicron particles of sparingly water-soluble drugs by precipitation in oil-in-water emulsions. I. Influence of emulsification and surfactant concentration" *J. Pharm. Sci.*, 82: 579–583, (1993)
12. B. Sjöström, B. Bergenstahl and B. Kronberg. "A method for the preparation of submicron particles of sparingly water-soluble drugs by precipitation in oil-in-water emulsions. II: Influence of the emulsifier, the solvent, and the drug substance" *J. Pharm. Sci.*, 82: 585–589, (1993)
13. J. R. Bellare, H. T. Davis, L. E. Scriven and Y Talmon. "Controlled environment vitrification system: an improved sample preparation technique" *J. Electron Microsc. Technique.* 10: 87–111 (1988)
14. T. M. Clausen, P. K. Vinson, J. R. Minter, H. T. Davis, Y. Talmon and W. G. Miller. "Viscoelastic micellar solutions: microscopy and rheoology" *J. Phys. Chem.* 96: 474–484 (1992)
15. D. Cochin, F. Candau, R. Zana and Y. Talmon. "Direct imaging of microstructures formed in aqueous solutions of polyamphiphiles" *Macromolecules*, 25: 4220–4223 (1992)
16. R. G. Laughlin, R. L. Munyon, J. L. Burns, T. W. Coffindaffer and Y. Talmon. "Physical science of the dioctadecyldimethylammonium chloride-water system. 3. Colloidal aspects" *J. Phys. Chem.*, 96: 373–383 (1992)
17. N. Kamenka, M. Chorro, Y. Talmon and R. Zana. "Study of mixed aggregates in aqueous solutions of sodium dodecylsulfate and dodecyltrimethylammonium bromide" *Colloids Surfaces*, 67: 213–222 (1992)
18. S. B. Dubin. *Methods Enzymol.* 26: 119–174 (1972)
19. B. Chu. "*Laser light scattering*" Academic Press 1991
20. F. Perrin. "Mouvement Brownien d"un ellipsoide I" *J. Phys. Radium* 5: 497–511 (1934)
21. F. Perrin. "Movement Brownien d'un ellipsoide II" *J. Phys. Radium* 7: 1–11 (1936)
22. B. Jacrot. "The study of biological structures by neutron scattering from solution" *Rep. Progr. Mod. Phys.* 39: 911–953 (1976)
23. A. Guinier and G. Fournet. "*Small Angle Scattering of X rays*" Wiley, New York 1955
24. O. Glatter and O. Kratky. *Small Angle X rays Scattering*", Academic Press 1982
25. B. Cabane. in R. Zana (ed.), "*Surfactant solutions: new methods of investigation*", M. Dekker, New York 1987 pp 57–145
26. M. J. Chapman. "Animal lipoproteins: chemistry, structure and comparative aspects" J. Lipid Res., 21: 789–853 (1980)
27. A. Walter, P. K. Vinson, A. Kaplun and Y. Talmon. "Intermediate structures in the cholate-phosphatidylcholine vesicle-micelle transition" *Biophys. J.* 60: 1315–1325 (1991)
28. Y. Talmon. "Imaging surfactant dispersions by transmission electron microscopy of vitrified specimens" *Colloids Surfaces* 19: 237–248 (1986)
29. W. C. Griffin. "Classification of surface active agents by HLB" *J. Soc. Cosmet. Chem.* 1: 311–326 (1949)
30. K. Shinoda and S. Friberg. "*Emulsions and Solubilization*", Wiley, New York 1986 pp 59–93